CHEMISTRY
A EUROPEAN JOURNAL

DOI: 10.1002/chem.200501199

Naturally Engineered Glycolipid Biosurfactants Leading to Distinctive Self-Assembled Structures

Tomohiro Imura,[a] Noboru Ohta,[b] Katsuaki Inoue,[b] Naoto Yagi,[b] Hideyuki Negishi,[a] Hiroshi Yanagishita,[a] and Dai Kitamoto*[a]

Abstract: Self-assembling properties of "natural" glycolipid biosurfactants, mannosyl-erythritol lipids A and B (MEL-A, MEL-B), which are abundantly produced from yeast strains, were investigated by using the fluorescence-probe method, dynamic light-scattering (DLS) analysis, freeze-fracture transmission electron microscopy (FF-TEM), and synchrotron small/wide-angle X-ray scattering (SAXS/WAXS) analysis, among other methods. Both MEL-A and MEL-B exhibit excellent self-assembly properties at extremely low concentrations; they self-assemble into large unilamellar vesicles (LUV) just above their critical-aggregation concentration (CAC). The CAC_I value was found to be 4.0×10^{-6} M for MEL-A and 6.0×10^{-6} M for MEL-B. Moreover, the self-assembled structure of MEL-A above a CAC_{II} value of 2.0×10^{-5} M was found to drastically change into sponge structures (L_3) composed of a network of randomly connected bilayers that are usually obtained from a complicated multicomponent "synthetic" surfactant system. Interestingly, the average water-channel diameter of the sponge structure was 100 nm. This is relatively large compared with those obtained from "synthetic" surfactant systems. In addition, MEL-B, which has a hydroxyl group at the C-4′ position on mannose instead of an acetyl group, gives only one CAC; the self-assembled structure of MEL-B seems to gradually move from LUV to multilamellar vesicles (MLV) with lattice constants of 4.4 nm, depending on the concentration. Furthermore, the lyotropic-liquid-crystal-phase observation at high concentrations demonstrates the formation of an inverted hexagonal phase (H_2) for MEL-A, together with a lamella phase (L_α) for MEL-B, indicating a difference between MEL-A and MEL-B molecules in the spontaneous curvature of the assemblies. These results clearly show that the difference in spontaneous curvature caused by the single acetyl group on the head group probably decides the direction of self-assembly of glycolipid biosurfactants. The unique and complex molecular structures with several chiral centers that are molecularly engineered by microorganisms must have led to the sophisticated self-assembling properties of the glycolipid biosurfactants.

Keywords: biosurfactants · glycolipids · self-assembly · sponge structures · vesicles

Introduction

The self-assembly of biologically based amphiphilic molecules into potentially useful structures has been the subject of intense study in recent years. Many types of amphiphilic molecules, such as lipids or proteins, self-assemble to form a wide variety of objects, including vesicles,[1] tubes,[2] and helical ribbons.[3] In most cases, the biological molecules have complicated structures, with one or more chiral centers and functional groups, which allow them to self-assemble into hierarchically ordered structures by using hydrogen bonding, and hydrophobic and van der Waals interactions.[4] However, the stereo- and regioselective synthesis of these complicated compounds is generally difficult, which has limited the widespread application of self-assembled biomaterials.

Biosurfactants are natural amphiphilic molecules that are abundantly produced from renewable resources by microorganisms. They have many advantages over their chemically synthesized counterparts, including their mild production conditions, and higher environmental compatibility and surface activity.[5] Although the physiological functions of biosurfactants are not clear, it has been suggested that microor-

[a] Dr. T. Imura, Dr. H. Negishi, Dr. H. Yanagishita, Dr. D. Kitamoto
Research Institute for Innovation in Sustainable Chemistry
National Institute of Advanced Industrial Science and Technology (AIST), Tsukuba Central 5-2, 1-1-1 Higashi
Tsukuba, Ibaraki 305-8565 (Japan)
Fax: (+81) 29-861-4660
E-mail: dai-kitamoto@aist.go.jp

[b] Dr. N. Ohta, Dr. K. Inoue, Dr. N. Yagi
Japan Synchrotron Radiation Research Institute (JASRI/Spring8)
1-1-1 Kouto, Mikazuki, Sayo, Hyogo 679-5198 (Japan)

ganisms secrete biosurfactants into the culture medium for emulsification of carbon sources such as vegetable oil or *n*-alkane.[6] This would promote the transport of the carbon sources across the cell wall and facilitate the growth of microorganisms.[7] Most of these functions are related to the amphipathic properties of biosurfactants. Typical hydrophilic groups of biosurfactants are carbohydrates and peptides, whereas typical hydrophobic groups are saturated or unsaturated fatty acids. The combination of these hydrophilic and hydrophobic groups and the whole structure of biosurfactants have been refined and optimized during the integration process of microbial evolution. Moreover, biosurfactants are stereo- and regioselectively synthesized by enzymatic reactions, and thus most of them are chiral compounds with a unified molecular configuration. However, despite these fascinating structural features of biosurfactants, only a few studies have been carried out on their self-assembled structure.[8]

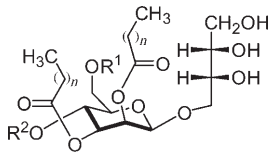

MEL-A: $R^1 = R^2 = Ac$
MEL-B: $R^1 = Ac$, $R^2 = H$
($n = 6$–10)

Figure 1. Structure of mannosyl-erythritol lipids (MELs).

Mannosyl-erythritol lipids (MELs, see Figure 1) are one of the most promising glycolipid biosurfactants.[9a] They are abundantly produced by yeast strains of *Pseudozyma antarctica* from soybean oil or *n*-alkane at a yield of up to 140 $g L^{-1}$.[9b] We have previously reported that MELs exhibit not only excellent surface activities[9c] but also a remarkable binding affinity toward human immunoglobulin G (HIgG).[9d] More recently, we revealed that the single component of MEL-A self-assembles into a sponge phase (L_3 phase), which is usually obtained from a complicated multicomponent system, together with giant vesicle formation of MEL-B at remarkably low concentrations.[9e] However, the ingenious contrivances of the self-assembly concealed in the complex and unique structure of MELs, which are molecularly engineered by nature, have not yet been clarified.

In this paper, we report for the first time the distinctive self-assembling properties of MEL-A and MEL-B revealed by the fluorescence-probe method, dynamic light-scattering (DLS) analysis, freeze-fracture transmission electron microscopy (FF-TEM), and synchrotron small/wide-angle X-ray scattering (SAXS/WAXS), among other methods. We also address the significance of biosurfactant production by microorganisms from a physiological perspective.

Results and Discussion

One of the most important properties of surfactants is to form aggregates such as micelles in aqueous solution. Determination of the critical-aggregation concentration (CAC) for glycolipid biosurfactants MEL-A and MEL-B was performed by using the pyrene fluorescence method.[10] The intensity ratio I_1/I_3 (see the Experimental Section) was used to determine the CAC of biosurfactants and to explore the refined structural change of the assemblies. Figure 2 shows the

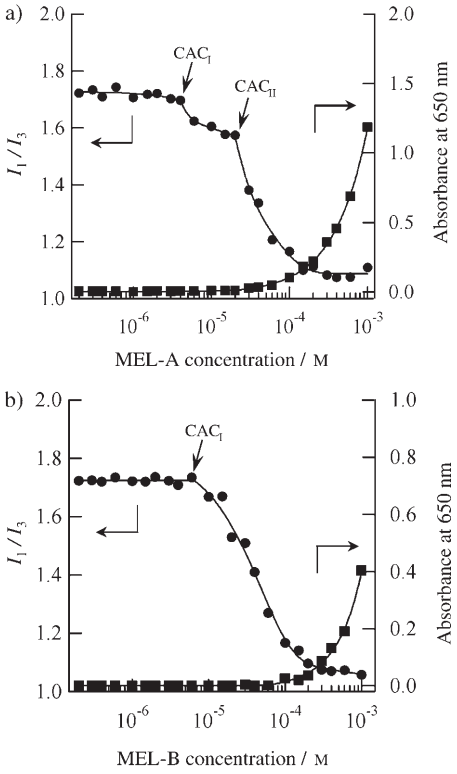

Figure 2. I_1/I_3 ratio of pyrene and absorbance at 650 nm of MEL solutions as a function of MEL concentration: a) MEL-A; b) MEL-B

variation of the I_1/I_3 ratio of the pyrene emission as a function of the MEL-A or MEL-B concentration. This figure also exhibits the absorbance of the biosurfactant solutions at 650 nm (turbidity). The I_1/I_3 ratio of the MEL-A solution gave an initial decay, at a remarkably low concentration of 4.0×10^{-6} M (CAC_I), from approximately 1.72, corresponding to pyrene placed in an aqueous environment,[10a] to 1.57. This indicates the formation of the MEL-A aggregate I above CAC_I, and pyrene is distributed into the hydrophobic domains of the aggregate. The I_1/I_3 ratio dropped further at a MEL-A concentration of 2.0×10^{-5} M (CAC_{II}) from a value of 1.57 to 1.08. The MEL-A solution then became turbid just above CAC_{II} as shown in the figure (see right axis), suggesting the formation of an aggregate II that is larger than aggregate I. These results indicate that MEL-A specifically gives two CACs, at 4.0×10^{-6} M (CAC_I) and 2.0×10^{-5} M (CAC_{II}), whereas our previously measured surface-tension data gave a single CAC at 2.7×10^{-6} M ($\gamma_{CAC}=28.4$ mN m^{-1}).[9c] This means that the fluorescence method is more sensitive than the surface-tension method. On the other hand, MEL-B, which has a hydroxyl group at the C-4′ position instead of an acetyl group, exhibited only one CAC at 6.0×10^{-6} M as shown in Figure 2b. The CAC_I value was almost the same as the value ($CAC_I=4.5\times10^{-6}$ M, $\gamma_{CAC}=$

28.2 mN m^{-1}) obtained from surface-tension measurements.[9c] The CAC_I value of MEL-A is slightly smaller than that of MEL-B because the hydrophobicity of MEL-A, which has an acetyl group at the C-4′ position, is higher than that of MEL-B, which has a hydroxyl group. These results clearly demonstrate that the difference in one functional group on the head group is likely to affect not only the CAC value but also the self-assembling behavior of MEL above the CAC.

To ascertain the size of MEL-A or MEL-B aggregates above CAC_I, dynamic light-scattering (DLS) measurements were performed at a low surfactant concentration of 1.0×10^{-5} M. Surfactants generally form spherical micelles above the critical micelle concentration (CMC), and the radius of the micelle is several nanometers, which almost equals its hydrophobic chain length.[11] Table 1 lists the dynamic light-scattering data obtained at a surfactant concentration above CAC_I (1.0×10^{-5} M). Surprisingly, huge aggregates were observed just above CAC_I, and their hydrodynamic diameters were found to be 179.0 nm for MEL-A and 161.9 nm for MEL-B. The obtained polydispersity indexes were 0.39 for MEL-A and 0.66 for MEL-B.[12] This clearly indicates that MEL-A and MEL-B do not self-assemble into micelles but into other kinds of structures just above the CAC_I. We also carried out the DLS measurements at a concentration above the CAC_{II}. However, the solutions at this concentration (1.0×10^{-3} M) were turbid, and the size of the aggregates was beyond the upper confidence limit of DLS detection (>1 μm).

Table 1. DLS data obtained at a surfactant concentration above CAC_I (1.0×10^{-5} M).

	Hydrodynamic diameter [nm]	Diffusion coefficient ($\times10^{-8}$) [cm^2 sec^{-1}]
MEL-A	179.0	2.78
MEL-B	161.9	3.06

The structures of the MEL-A and MEL-B assemblies were then determined by using a freeze-fracture transmission electron microscope (FF-TEM). Figure 3A and B show typical freeze-fracture electron micrographs of assembled MEL-A and MEL-B structures at a concentration of 1.0×10^{-5} M. The figures indicate that both MEL-A and MEL-B do not self-assemble into micelles but into large unilamellar vesicles (LUV) whose diameters are almost equal to those obtained from DLS measurements above CAC_I. This means that both biosurfactants exhibit an excellent self-assembling property at an extremely low concentration of 1.0×10^{-5} M. Moreover, the self-assembled structure of MEL-A above CAC_{II} was found to drastically change as shown in Figure 3C, which shows a typical freeze-fracture electron micrograph of assembled MEL-A structures at the concentration of 1.0×10^{-3} M. The figure clearly exhibits the typical morphology of a sponge structure (L_3 phase) composed of a randomly connected three-dimensional network of the bilayers[13] as drawn in Figure 4. In Figure 3C, the spherical and ellipsoidal objects with a planar appearance are the water domains because the fracture through the water phase occurs perpendicular to the curved bilayers. In many parts of the micrograph we can follow the bilayer over a range of several micrometers, which indicates that the bilayer is indeed continuous. In places where the fracture occurred along two bilayers, a bilayer with both a negative and a positive spontaneous curvature can be seen. The observed drastic change in the self-assembled structures from large unilamellar vesicles (LUV) to sponge structures (L_3 phase) is found to provide two CACs for MEL-A. The freeze-fracture electron micrograph of the assembled MEL-B structure at the concentration of 1.0×10^{-3} M gives typical multilamellar-vesicle (MLV) morphology as we previously reported.[9e] The self-assembled structure of MEL-B seems to gradually move from LUV to MLV depending on the concentration, which would result in only one CAC for MEL-B. These results clearly demonstrate that the single acetyl group on the

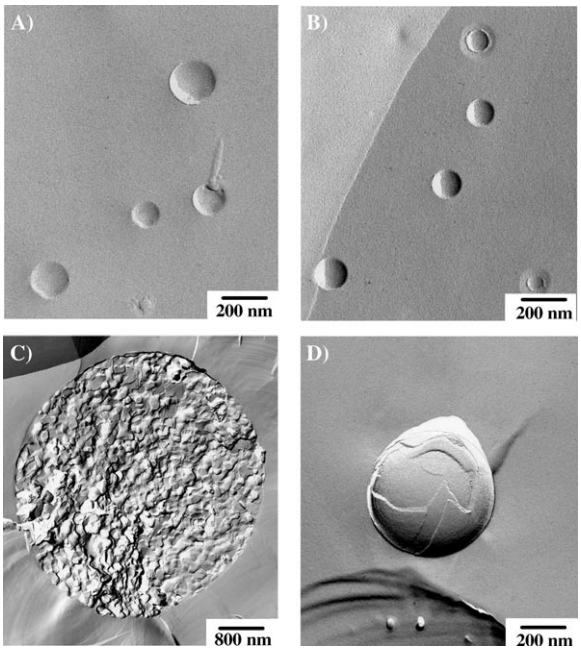

Figure 3. Freeze-fracture transmission electron micrographs of MEL-A [A) 1.0×10^{-5}, C) 1.0×10^{-3} M] and MEL-B [B) 1.0×10^{-5}, D) 1.0×10^{-3} M] assemblies.

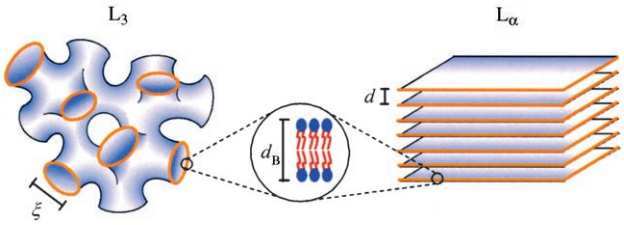

Figure 4. Schematic representation of sponge (L_3) and lamellar structures (L_α) and their respective characteristic lengths, sponge pore size (ξ), and lamellar periodicity (d). The inset shows an expanded view of a section of the membrane displaying the assembly of MEL molecules forming a bilayer of thickness d_B.

head group decides the direction of self-assembly; this causes the drastic difference in self-assembled structures.

Among the variety of surfactant aggregates, the sponge phase (L_3) is a relatively new class of surfactant assemblies, which are usually obtained from complicated multicomponent systems such as surfactants with salt/cosolvent.[13] The sponge-phase (L_3) formation from a single component of "synthetic" zwitterionic gemini surfactant was reported by Menger and co-workers.[14] This is the first observation of sponge-phase (L_3) formation from a single component of "natural" glycolipid biosurfactant (MEL-A) even though it possesses different alkyl-chain lengths (C8 to C12). It is truly remarkable that the single component of MEL-A, a major component of yeast products, self-assembles into a sponge phase (L_3) at an extremely low concentration. Here, let us discuss the prospective physiological significance of biosurfactant production by the yeast strains of *Pseudozyma antarctica*. It is well known that assembled lipid structures, especially bicontinuous cubic structures, play a significant role in biological systems:[15] the bicontinuous cubic structures appear during the hydrolysis of triglycerides and facilitate the lypolysis process by markedly enhancing lipase activity. Monoglycerides such as monoolein, obtained from the hydrolysis of triglycerides, are experimentally found to self-assemble into bicontinuous cubic structures. The sponge phase (L_3) also has a bicontinuous structure and is recognized as a melted cubic phase, obviously lacking long-range order.[16] A low-viscosity sponge phase will be more effective for lipase activity than a stiff cubic phase. Moreover, yeast strains of *Pseudozyma antarctica* abundantly secrete lipase as well as MEL-A into the culture medium. Although the physiological significance of biosurfactants remains ambiguous, these lines of evidence possibly suggest that yeast strains of *Pseudozyma antarctica* might produce them not only to emulsify carbon sources but also to provide a self-assembled sponge structure as a reaction field that can greatly enhance lipase activity.

We further investigated the structure of the naturally occurring sponge phase (L_3 phase) obtained from MEL-A by using synchrotron small-angle X-ray scattering (SAXS) and wide-angle X-ray scattering (WAXS) analyses. We also approached the detailed mechanism of the drastic structural difference between the sponge phase (L_3) and the multilamellar vesicle (L_α), caused by the single acetyl group on the head group.

Figure 5a shows the small-angle diffractograms of assembled MEL-A and MEL-B structures and the drastic difference in the scattering behavior between the two can be clearly seen. Whereas the scattering curve of the MEL-A assembly has a broad peak at 0.35 nm^{-1}, the scattering curve of the MEL-B assembly gives two sharp peaks at 0.22 and 0.44 nm^{-1}, respectively. The diffractogram of the MEL-B assembly consists of two peaks and clearly indicates a lamella structure (L_α), and the obtained lattice constant (d) is 4.4 nm. The broad peak obtained from the MEL-A assembly is similar to the previously reported scattering curve of a typical sponge phase (L_3) composed of a randomly connected three-dimensional network of bilayers.[17] Our peak fitting, performed according to recently described algorithms,[18] yielded a bilayer thickness (d_B) of 3.2 nm for both MEL-A and MEL-B, as drawn in Figure 4. Moreover, the average water-channel diameter (ξ) was found to be about 100 nm from FF-TEM observation. Another peak of the MEL-A assembly observed below 0.17 nm^{-1} might be caused by the water channel of the sponge structure. Interestingly, the water-channel diameter of the "natural" biosurfactant sponge phase seems to be larger than that of the "synthetic" surfactant:[19] the reported water-channel diameter with a "synthetic" surfactant multicomponent system (cetylpyridinium/hexanol/dextrose/brine) was about 24 nm. The wide-angle diffractograms of the assembled MEL-A and MEL-B structures are shown in Figure 5b. The broad bands at high angles (arrows: $S = 2.2$ nm^{-1}) in Figure 5b indicate that the alkyl chains of both MEL-A and MEL-B are in the liquid state at room temperature (25 °C) due to their medium-alkyl-chain length (C8 to C12).[20]

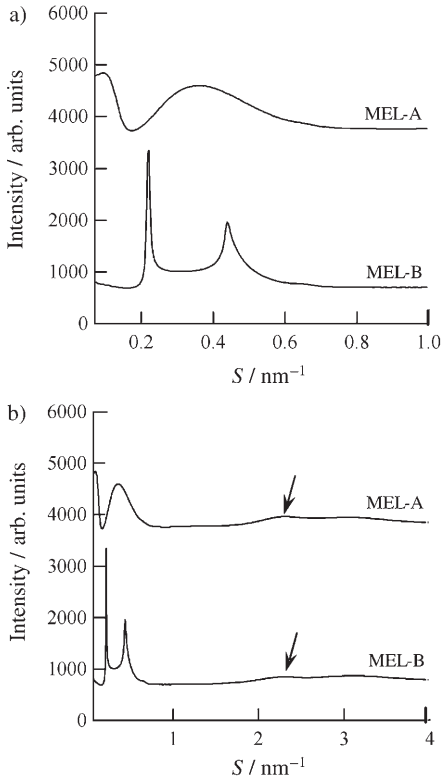

Figure 5. Synchrotron a) SAXS and b) WAXS curves of MEL-A and MEL-B assemblies.

Theoretically, the sponge phase (L_3) appears when the spontaneous curvature is slightly negative.[16b] Spontaneous curvature (H_0) is a useful parameter to characterize assembled lipid structures. It is given by $H_0 = 1/R_0$, in which H_0 is the curvature of a single monolayer and R_0 is the spontaneous radius of curvature.[21] When the spontaneous curvature is nearly zero, the lipids self-assemble into the lamella phase (L_α). To ascertain the spontaneous curvature of biosurfactants temporarily, a water-penetration scan was performed

to observe the lyotropic-liquid-crystalline phases for MEL-A and MEL-B. The difference in spontaneous curvature between the two probably causes the difference in the lyotropic-liquid-crystalline structure. Figure 6A shows the photographs for MEL-A with increasing concentration from left to right. The upper photograph in Figure 6A without crossed polarizers clearly indicates five different regions that should represent water (W), the L_3 phase (L_3), the inverted cubic phase (V_2), the inverted hexagonal phase (H_2), and the neat surfactant phase (S). The lower photograph in Figure 6A with crossed polarizers clearly shows an inverted hexagonal morphology[22] (H_2) next to the neat surfactant phase (S); this indicates that the spontaneous curvature of the MEL-A assemblies is negative. Figure 6B shows the results for MEL-B. Once in contact with water, myelin figures immediately formed and grew into elongated tubes. The four different regions are shown in Figure 6B, which represents water (W), myelines, the lamella phase (L_α), and the neat surfactant phase (S), and indicate that the spontaneous curvature of MEL-B assemblies is almost zero. Although SAXS measurements are required to determine the detailed structure of the lyotropic-liquid-crystalline structure, these observations clearly indicate that the single acetyl group on the head group induces the difference in the spontaneous curvature, which causes the drastic change in phase behavior between MEL-A and MEL-B. That a single acetyl group on the head group decides the direction of self-assembly is truly remarkable. This is very likely to arise from the highly sophisticated structure of glycolipid biosurfactants, which are stereo- and regioselectively synthesized by enzymatic reactions. Interestingly, the other known glycolipid biosurfactants such as rhamnolipids (RL) and sophorolipids (SL) also self-assemble into a variety of structures, and their assembled structures change drastically with slight variation in the head group. Because of the carboxylic acid on the head groups, RLs reversibly change their self-assembled structures from vesicles to lipid particles and finally to micelles within a narrow pH range of about 5–7.[8a] SLs also self-assemble into giant twisted and helical ribbons of 5–11 μm width and several hundreds of micrometers in length in acidic conditions ($pH < 5.5$). Increase in the solution pH values decreased the ribbon yield and increased the helicity and entanglements of the giant ribbons.[8b]

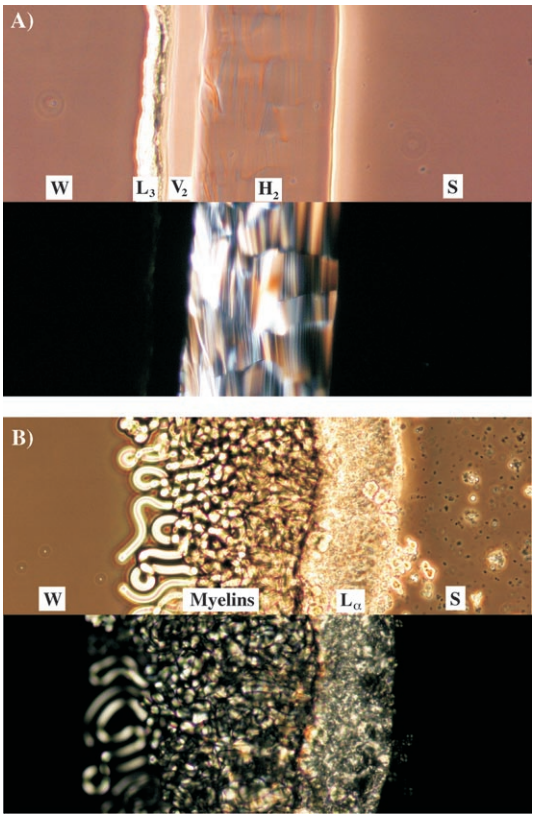

Figure 6. Water penetration scans of A) MEL-A and B) MEL-B viewed with and without crossed-polarizing filters.

In addition, we have recently reported that glycolipid biosurfactants MEL-A and MEL-B exhibit an excellent molecular-recognition ability toward useful proteins such as HIgG through the "multivalent effect".[9d] It is well known that membrane glycolipids such as ganglioside and glycosphingolipids also exhibit a high affinity to HIgG.[23] The potential application of these glycolipid assemblies for protein separation or as delivery materials is, however, far from straightforward owing to their limited amounts and heterogeneity.[24] On the other hand, the present unique self-assembled structures obtained from MEL-A or MEL-B would be useful for protein materials because they are so-called "glycoclusters" with high surface areas that promise a multivalent effect. Furthermore, the microbial glycolipid biosurfactant can be produced abundantly compared with membrane glycolipids. In particular, another essential aspect for sponge structures is the determination of the critical capacity of proteins in the water channels of the assembled structures. Glycolipid biosurfactants should thus open new avenues for the development of novel nanobiomaterials.

Conclusion

In this work, we report the self-assembling properties of "natural" glycolipid biosurfactants MEL-A and MEL-B, which are molecularly engineered by microorganisms. Both MEL-A and MEL-B exhibit an excellent self-assembling property at extremely low concentrations. Whereas MEL-A, which has an acetyl group at the C-4′ position on the head group, exhibits two critical-aggregation concentrations (CACs), MEL-B, which has a hydroxyl group at the C-4′ position, has only one CAC. MEL-A self-assembles into large unilamellar vesicles (LUV) just above CAC_I, and then drastically changes its self-assembled structure into sponge structures (L_3) above CAC_{II}. Moreover, the average water-channel diameter of the sponge structure was about 100 nm, which seems to be larger than that of sponge structures obtained from "synthetic" surfactant systems. Meanwhile,

MEL-B also self-assembles into LUV above CAC_I and then gradually grows to a multilamellar vesicle (MLV) depending on the concentration. At high concentrations, the formation of an inverted hexagonal phase (H_2) for MEL-A and a lamella phase (L_α) for MEL-B was clearly observed by polarized microscopy. The present study thus reveals the ingenious contrivances of the self-assembly concealed in the unique molecular structure of MEL: the single acetyl group on the head group dominates the spontaneous curvature of assembly, which directly decides the direction of self-assembly of glycolipid biosurfactants.

It is remarkable that microorganisms like yeast strains outwardly secrete such biosurfactants with an excellent self-assembling ability. Although the physiological significance of biosurfactants is still a scientific mystery, microorganisms might produce biosurfactants not only to emulsify carbon sources but also to provide elegant self-assembled structures leading to greatly enhanced enzymatic reactions, because we believe that there is no waste in biological and physical cycles in nature.

Experimental Section

Materials: 4-*O*-(4′,6′-Di-*O*-acetyl-2′,3′-di-*O*-alkanoyl-β-D-mannopyranosyl)-D-erythritol (MEL-A) and 4-*O*-(6′-*O*-acetyl-2′,3′-di-*O*-alkanoyl-β-D-mannopyranosyl)-D-erythritol (MEL-B) were used as glycolipid biosurfactants. MEL-A and MEL-B were obtained by the following procedure: A seed culture (1.5 mL) of the yeast strain *Pseudozyma antarctica* was transferred to 300 mL Erlenmeyer flasks containing 30 mL of a fermentation medium [4% (v/v) soybean oil, 0.2% $NaNO_3$, 0.02% $MgSO_4{\cdot}7H_2O$, 0.02% KH_2PO_4, 0.1% yeast extract, distilled water], and incubated on a rotatory shaker (220 rpm) at 30°C for one week. The culture broth (30 mL) was then extracted twice with 30 mL portions of ethyl acetate. The layer was separated, and the organic layer was washed with brine and concentrated under reduced pressure. The resulting yellow oil (555 mg) was dissolved in chloroform (5 mL) and placed on a column (3×40 cm) of silica gel (50 g). The crude MELs have a composition of 80% MEL-A and 20% MEL-B. The mixture of MELs was then subjected to chromatography with a close-gradient elution of chloroform/acetone (10:0 to 0:10). Each fraction was collected and again subjected to chromatography as described above to give MEL-A and MEL-B. They have a fatty acid composition of 18% C8, 71% C10, and 11% C12. The characterization of MEL-A or MEL-B is given in the Supporting Information of ref. [9a]. The purified MEL-A or MEL-B was dissolved in acetone, and the stock solution was transferred into a test tube. After the solvent was removed by using a rotary evaporator, distilled water was added to the test tube. The MEL-A or MEL-B solution was obtained by placing the test tube under vortex conditions for one minute at room temperature (25°C).

Fluorescence measurements: The critical-aggregation concentration (CAC) of the biosurfactant solutions was determined by using pyrene fluorescence at 25°C.[10] Pyrene is a hydrophobic molecule with a low aqueous solubility and is solubilized in the hydrophobic domains of surfactant aggregates. The fluorescence spectrum of pyrene is related to its vibronic fine structure, and the relative peak intensity is strongly dependent on the polarity of the microenvironment. With increasing polarity, the intensity of the first band (I_1) is enhanced, whereas no effect is observed on the intensity of the third band (I_3). The characteristic intensity ratio, I_1/I_3, was measured as a function of the biosurfactant concentration with an FP-6500 spectrofluorometer (JASCO Co., Japan). Excitation of the pyrene probe was performed at 335 nm, and the detection wavelengths were 373 nm for I_1 (first peak) and 384 nm for I_3 (third peak). The thin pyrene films were prepared by transferring a sufficient amount of a methanol-based stock solution of pyrene to test tubes under a stream of nitrogen, after which the biosurfactant solution was added. The final pyrene concentration was 5×10^{-7} M. The samples were incubated in the dark for 24 h at 25°C before measurements were taken.

Turbidity measurements: The turbidity of the biosurfactant solutions was performed by using a U-2800 UV/Vis spectrophotometer (Hitachi High-Technology Co., Japan) at a wavelength of 650 nm in quartz sample cells (1 cm thick) at 25°C.

Dynamic light scattering (DLS): The size of the assembled structures was measured with a DLS-7000 instrument (Otsuka Electronics Co., Japan) using a He-Ne laser of 633 nm wavelength as a light source at 25°C. The time-dependent correlation function of the scattered-light intensity was measured at a scattering angle of 90°. The DLS intensity data were processed by using the instrumental software to obtain the hydrodynamic diameter, the polydispersity index, and the mass-diffusion coefficient of the samples. The mass-diffusion coefficient (D) was derived from the decay time (τ_C) of the intensity autocorrelation function using $D=(2k_L^2\tau_C)^{-1}$, in which k_L is the scattering wave vector. The hydrodynamic mass-diffusion coefficient D_0 is obtained as the limit of D as k_L goes to zero. D_0 is found to obey the Stokes–Einstein relation, $D_0=kT/6\pi\eta R_H$, in which k is the Boltzmann constant, T is the absolute temperature, η is the viscosity of the solution, and R_H is the hydrodynamic radius. In this study, the autocorrelation function was analyzed by using the cumulant method.[25]

Freeze-fracture electron microscopy (FFEM): Freeze-fracture electron microscopy was used to determine the structure of the assemblies. Some samples were frozen with liquid nitrogen at −189°C. The fracture process was performed with a JFD-9010 instrument (JOEL, Japan) at −130°C and the fractured surface was then replicated by evaporating platinum at an angle of 60°, followed by carbon at an angle of 90° to strengthen the replica. The replicate was placed on a copper grid (400 mesh) after being washed with water, methanol, and chloroform. It was then examined and photographed by using a JEM-1010 (JOEL, Japan) transmission electron microscope.

Synchrotron X-ray scattering: Small-angle and wide-angle X-ray scattering (SAXS/WAXS) experiments were performed with the optics and detector system installed at BL-40B2 (Structural Biology II Beamline) of the synchrotron radiation facility SPring-8, Hyogo, Japan. The details of the beamline have been described in ref. [26a]. The wavelength (λ) of the incident X-ray beam was 0.083 nm. An imaging-plate area detector R-AXIS IV (Rigaku, Japan) was used to detect the scattered X-ray signal. The distance between the sample and detector was about 400 mm. The reciprocal spacing $S=(2/\lambda)\sin(2\theta/2)$, in which 2θ is the scattering angle, was calibrated by the spacing of silver behenate at room temperature.[26b] The biosurfactant solutions (20 mM) were subject to centrifugation at 12000 rpm for 3 min, and the obtained lower phases were sealed into capillaries. The experimental data were measured at room temperature. The exposure time was 30 s.

Polarized optical microscopy: A polarized optical microscope (ECLIPSE E600, Nikon, Japan) with crossed-polarizing filters equipped with a charge-coupled-device camera (DS-SM, Nikon, Japan) was used to observe the lyotropic-liquid-crystalline phase of the biosurfactants. A halogen lamp (100 W) was used as a light source. The pictures were obtained with a ×100 objective lens with a numerical aperture of 0.3. Lyotropic-liquid-crystalline-phase behavior was investigated by using the water-penetration scan technique. Birefringent textures from the optical microscopy allowed the assignment of the particular lyotropic-phase types to the samples.

Acknowledgements

We would like to gratefully acknowledge Dr. Shinji Kohara of the Japan Synchrotron Radiation Research Institute (JASRI), SPring8, for encouraging this study and for providing useful suggestions. This study was supported by the Industrial Technology Research Grant Program in 05A33008c from the New Energy and Industrial Technology Development Organization (NEDO) of Japan.

[1] a) T. Baumgart, S. T. Hess, W. W. Webb, *Nature* **2003**, *425*, 821–824; b) T. Imura, T. Gotoh, K. Otake, S. Yoda, Y. Takebayashi, S. Yokoyama, H. Takebayashi, H. Sakai, M. Yuasa, M. Abe, *Langmuir* **2003**, *19*, 2021–2025; c) K. Otake, T. Imura, H. Sakai, M. Abe, *Langmuir* **2001**, *17*, 3898–3901; d) T. Imura, H. Sakai, H. Yamauchi, C. Kaise, K. Kozawa, S. Yokoyama, M. Abe, *Colloids Surf. B* **2001**, 20, 1–8.

[2] a) T. Shimizu, M. Masuda, H. Minamikawa, *Chem. Rev.* **2005**, *105*, 1401–1443; b) J. F. Graveland-Bikker, R. Ipsen, J. Otte, C. G. de Kruif, *Langmuir* **2004**, *20*, 6841–6846; c) A. Karlsson, R. Karlsson, M. Karlsson, A.-S. Cans, A. Strömberg, F. Ryttsén, O. Orwar, *Nature* **2001**, *409*, 150–152.

[3] a) L. Moreau, P. Barthélémy, M. E. Maataoui, M. W. Grinsraff, *J. Am. Chem. Soc.* **2004**, *126*, 7533–7539; b) M. S. Spector, A. Singh, P. B. Messersmith, J. M. Schnur, *Nano Lett.* **2001**, *1*, 375–378.

[4] a) G. M. Whitesides, B. Crzybowski, *Science* **2002**, *295*, 2418–2421; b) J. J. L. M. Cornelissen, A. E. Rowan, R. J. M. Nolte, N. A. J. M. Sommerdijk, *Chem. Rev.* **2001**, *101*, 4039–4070.

[5] a) "Glycolipid-Based Bionanomaterials": D. Kitamoto, K. Toma, M. Hato in *Handbook of Nanostructured Biomaterials and Their Applications in Nanobiotechnolgy, Vol. 1* (Ed.: H. S. Nalwa), American Scientific, Los Angeles, **2005**, pp. 239–271; b) S.-C. Lin, *J. Chem. Technol. Biotechnol.* **1996**, *66*, 109–120; c) I. M. Banat, *Bioresour. Technol.* **1995**, *51*, 1–12.

[6] a) C. N. Mulligan, *Environ. Pollut.* **2005**, *133*, 183–198; b) G. Bognolo, *Colloids Surf. A* **1999**, *152*, 41–52.

[7] a) R. Hommel, O. Stüwer, W. Stuber, D. Haferburg, H.-P. Kleber, *Appl. Microbiol. Biotechnol.* **1987**, *26*, 199–205; b) K. Hisatsuka, T. Nakahara, N. Sano, K. Yamada, *Agric. Biol. Chem.* **1971**, *35*, 686–692.

[8] a) Y. Ishigami, Y. Gama, H. Hagahora, M. Yamaguchi, H. Nakahara, T. Kamata, *Chem. Lett.* **1987**, 763–766; b) S. Zhou, C. Xu, J. Wang, W. Gao, R. Akhverdiyeva, V. Shah, R. Gross, *Langmuir* **2004**, *20*, 7926–7932; c) A. Abalos, A. Pinazo, M. R. Infante, M. Casals, F. Garcia, A. Manresa, *Langmuir* **2001**, *17*, 1367–1371.

[9] a) D. Kitamoto, S. Ghosh, Y. Nakatani, G. Ourisson, *Chem. Commun.* **2000**, 861–862; b) D. Kitamoto, T. Ikegami, T. Suzuki, A. Sasaki, Y. Takeyama, Y. Idemoto, N. Koura, H. Yanagishita, *Biotechnol. Lett.* **2001**, *23*, 1709–1714; c) D. Kitamoto, H. Isoda, T. Nakahara, *J. Biosci. Bioeng.* **2002**, *94*, 187–201; d) J.-H. Im, H. Yanagishita, T. Ikegami, D. Kitamoto, *J. Biomed. Mater. Res.* **2003**, *65*, 379–385; e) T. Imura, H. Yanagishita, D. Kitamoto, *J. Am. Chem. Soc.* **2004**, *126*, 10804–10805.

[10] a) K. C. Hoang, S. Mecozzi, *Langmuir* **2004**, *20*, 7347–7350; b) J. H. Mathias, *Langmuir* **2001**, *17*, 6148–6154; c) D. S. Yin, W. Y. Yang, Z. Q. Ge, Y. J. Yuan, *Carbohydr. Res.* **2005**, *340*, 1201–1206; d) E. T. Iamazaki, C. C. Schmitt, M. G. Neumann, *Langmuir* **2001**, *17*, 3486–3490.

[11] a) Y. Kondo, H. Miyazawa, H. Sakai, M. Abe, N. Yoshino, *J. Am. Chem. Soc.* **2002**, *124*, 6516–6517; b) T. Yoshimura, K. Esumi, *Langmuir* **2003**, *19*, 3535–3538; c) F. Bockstahl, E. Pachoud, G. Duplâtre, I. Billard, *Chem. Phys.* **2000**, *256*, 307–313.

[12] a) M. Oishi, S. Sasaki, Y. Nagasaki, K. Kataoka, *Biomacromolecules* **2003**, *4*, 1426–1432; b) S. Sen, D. Sukul, P. Dutta, K. Bhattacharyya, *J. Phys. Chem. B* **2002**, *106*, 3763–3769; c) H. Yajima, H. Yamamoto, M. Nagaoka, K. Nakazato, T. Ishii, N. Niimura, *Biochim. Biophys. Acta* **1998**, *1381*, 68–76.

[13] a) A. Zapf, U. Hornfeck, G. Platz, H. Hoffmann, *Langmuir* **2001**, *17*, 6113–6118; b) R. Strey, W. Jahn, G. Porte, P. Bassereau, *Langmuir* **1990**, *6*, 1635–1639; c) H. Hoffmann, C. Thunig, U. Munkert, *Langmuir* **1992**, *8*, 2629–2638.

[14] a) A. V. Peresypkin, F. M. Menger, *Org. Lett.* **1999**, *1*, 1347–1350; b) F. M. Menger, A. V. Peresypkin, K. L. Caran, R. P. Apkarian, *Langmuir* **2000**, *16*, 9113–9116; c) F. M. Menger, A. V. Peresypkin, *J. Am. Chem. Soc.* **2001**, *123*, 5614–5615.

[15] a) R. Wallin, T. Arnebrant, *J. Colloid Interface Sci.* **1994**, *164*, 16–20; b) F. Caboi, J. Borné, T. Nylander, A. Khan, A. Svendsen, S. Patkar, *Colloids Surf. B* **2002**, *26*, 159–171.

[16] a) B. Balinov, U. Olsson, O. Söderman, *J. Phys. Chem.* **1991**, *95*, 5931–5936; b) D. Anderson, H. Wennerström, U. Olsson, *J. Phys. Chem.* **1989**, *93*, 4243–4253; c) A. Ridell, K. Ekelund, H. Evertsson, S. Engström, *Colloids Surf. A* **2003**, *228*, 17–24.

[17] a) M. Magalhães, A. M. Figueiredo Neto, A. C. Tromba, *J. Phys. Chem. B* **2004**, *108*, 15962–15968; b) N. Tsapis, R. Ober, A. Chaffotte, D. E. Warschawski, J. Everett, J. Kauffman, P. Kahn, M. Waks, W. Urbach, *Langmuir* **2002**, *18*, 4384–4392; c) M. Antonietti, C. Burger, M. A. Micha, M. Weissenberger, *Macromol. Chem. Phys.* **1999**, *200*, 150–155; d) H. F. Mahjoub, C. Bourgaux, P. Sergot, M. Kleman, *Phys. Rev. Lett.* **1998**, *81*, 2076–2079.

[18] a) G. Pabst, J. Katsaras, V. A. Raghunathan, M. Rappolt, *Langmuir* **2003**, *19*, 1716–1722; b) G. Pabst, M. Rappolt, H. Amenitsch, P. Laggner, *Phys. Rev. E* **2000**, *62*, 4000–4009.

[19] a) L. Porcar, W. A. Hamilton, P. D. Butler, *Langmuir* **2003**, *19*, 10779–10794.

[20] M. Magalhães, D. Pusiol, M. E. Ramia, A. M. Figueiredo Neto, *J. Chem. Phys.* **1998**, *108*, 3835–3843.

[21] Y. Aota-Nakano, S. J. Li, M. Yamazaki, *Biochim. Biophys. Acta* **1999**, *1461*, 96–102.

[22] a) M. Hato, I. Yamashita, T. Kato, Y. Abe, *Langmuir* **2004**, *20*, 11366–11373; b) M. Hato, H. Minamikawa, R. A. Salkar, S. Matsutani, *Langmuir* **2002**, *18*, 3425–3429.

[23] a) P. Boullanger, *Top. Curr. Chem.* **1997**, *87*, 275–312; b) S. V. Evans, C. R. Mackenzie, *J. Mol. Recognit.* **1999**, *12*, 155–168.

[24] T. Feizi, *Immunol. Rev.* **2000**, *173*, 79–88.

[25] a) J. Pencer, F. R. Hallett, *Langmuir* **2003**, *19*, 7488–7497; b) D. G. Hunter, B. J. Frisken, *Biophys. J.* **1998**, *74*, 2996–3002.

[26] a) K. Miura, M. Kawamoto, K. Inoue, M. Yamamoto, T. Kumasaka, M. Sugiura, A. Yamano, H. Moriyama, *SPring-8 User Experiment Report, Vol. 4*, **2000**, p. 168; b) T. C. Huang, H. Toraya, T. N. Blanton, Y. Wu, *J. Appl. Crystallogr.* **1993**, *26*, 180–184.

Received: September 29, 2005
Published online: December 23, 2005

